

Assessment of wood utility poles' deterioration through natural frequency measurements

Laura V. González de Paz^{1,2} · Néstor F. Ortega^{1,2} · Marta B. Rosales^{1,3}

Received: 28 April 2018 / Accepted: 1 November 2018 / Published online: 20 November 2018
© Springer-Verlag GmbH Germany, part of Springer Nature 2018

Abstract

Utility poles in a power distribution line are usually made of prestressed concrete, reinforced concrete or wood. In Latin America, given the abundance of different species of wood suitable for structural purposes, the latter material is more commonly used. The durability of wood in structures exposed to meteorological agents is usually an issue, especially when these have a critical role in the operation of industries or when the structures provide a service to society. For this reason, it is convenient to develop simple techniques that allow the assessment of the damage during their service life. In this paper, results obtained experimentally are contrasted with the outcomes of finite element models, taking deterministic property values of the material and simulating the same load state of the test. The correlation between the degree deterioration of wood poles and their dynamic behavior taking into account defects such as cracks, knots and others, was evaluated. The wood used in the experiments is *Eucalyptus grandis*, a species that is widely cultivated in South and Central America and particularly, found in the northeastern part of Argentina. The experimental work has been carried out in laboratory using real poles with different degrees of damage and deterioration, that were provided by the EDES, the electricity company that provides service in the Province of Buenos Aires, Argentina.

Keywords Wood poles · Wood damage · FEM · Experimental mechanics · Structural dynamics

1 Introduction

Utility poles made of timber are widely used all over the world because they are of relatively low cost and environmentally friendly. Apart from being a renewable resource, round wood also gives a very good ecological balance, because sawing is not needed and the use of primary energy is minimized. Consequently, the use of this

type of structures is also convenient for taking care of environmental aspects.

Eucalyptus grandis is a wood mainly cultivated in the Mesopotamian provinces of Entre Ríos and Corrientes, Argentina, and it is one of the most important renewable species cultivated in South America. It is extensively used in Argentina for structural purposes, in particular, utility poles.

Some standards indicate the procedures to determine the mechanical properties of wood [1] and [2], and particularly of wood poles [3]. Nevertheless, the deterioration, both natural and generated by environmental agents, has a direct effect on the rigidity and strength of these structural elements, and the values result in being different from those initially considered in the design.

Experimental studies are usually carried out to assess its properties and behavior [4] and more recently, computational approaches are reported in [5] and [6]. An experimental assessment of *Eucalyptus grandis* wood poles' mechanic properties and the knots' presence in the wood is present in [7].

✉ Laura V. González de Paz
lv.gdepaz@gmail.com

Néstor F. Ortega
nfortega@criba.edu.ar

Marta B. Rosales
mrosales@criba.edu.ar

¹ Department of Engineering, Universidad Nacional del Sur, Av. Alem 1253, Bahía Blanca, Argentina

² Instituto de Ingeniería, UNS-CIC (Buenos Aires), Bahía Blanca, Argentina

³ IFISUR, UNS-CONICET, Bahía Blanca, Argentina

There are a variety of environmental and material parameters that influence the deterioration of timber. The reference [8] presents a series of studies on monitoring of timber structures from a European perspective. In [9], a numerical study of the influence of different types of damage over the load capacity of in-service timber poles are presented. In [10], a study about damage quantification of wooden utility poles is presented taking into account wind load, variation in geometry and deterioration due to aging.

In the present work, a relationship between general deterioration and rigidity is sought through the measurement of different parameters: presence of knots, cracks, and density. The aim is to develop a method that allows a control of the in-service wood utility poles.

2 Methods and materials

The test sample consisted of six impregnated real-sized poles, five of which showed different degrees of deterioration after a period of service, and a last one without deterioration and without use. They were provided by the electricity company, Empresa Distribuidora de Energía del Sur (EDES). A geometrical survey was carried out on the sample. The actual length and circumference at base, at tip, at ground line, at the loading point and at every 0.60 m from the base were measured and recorded for each pole. It should be noted that after the clamping, the free length resulted in 5 m for all the poles. Table 1 depicts the main geometry data of the six poles.

2.1 Knots and other defects measurement

In accordance with the criterion adopted by the American standard [11], the dimension of a knot was measured and this was considered equal to its diameter on the surface of the pole measured in a direction at right angles to the

lengthwise axis of the pole. Dimension and location of all knots were taken and recorded.

The knot ratio was expressed for each pole according to the following criterion: relation of the greatest sum of knots in any 0.45 m of the length of the pole and the average circumference of the same 0.45 m section (SuKR). No distinctions were made between different types of knots, and those with diameters less than 15 mm were ignored. Likewise, a record of the visible cracks greater than 2 mm was taken and the ratio of the sum of the cracks (SuCR) was calculated with respect to the average circumference in sections every 0.45 m over the length of the pole.

2.2 Natural frequencies measurements

On the other hand, before carrying out the load-displacement test, the first three natural frequencies were measured experimentally. For the experimental determination of the frequencies, a modal impact test was carried out, by hitting the pole with a rubber hammer and recording the accelerations with accelerometer sensors placed on the tip of each pole. This location is optimal for the first frequency measurement, however, as it is not coincident with any node, it was adopted for the measurement of the remaining frequencies. From the acceleration time signal, the frequencies were obtained through a fast Fourier transform (FFT) of the record. These results were compared with those obtained from the numerical models that represent the same test.

A Vernier LabQuest™ interface [12] was used to record the acceleration. A 3-axis accelerometer was employed for acceleration values between $\pm 49 \text{ m/s}^2$ according to three orthogonal axes with frequency response between 0 and 100 Hz (Fig. 1). The vibration of the pole was induced by a sudden strike from its static equilibrium state applied with a rubber hammer at the free end. Accelerations were registered with a sensor on the pole tip, so that it does not coincide with a node of the element structural. Using a USB connection, the Vernier LabQuest™ was linked to a laptop where the Logger Pro software was installed. The data was collected at a rate of

Table 1 Main geometry data of the poles

Pole	Circumference at ground line at		Length (m)
	5 m from tip (mm)	Tip (mm)	
1	435	347	6.3
2	510	542	5.9
3	445	352	6.5
4	515	447	6.0
5	540	475	6.1
6	547	449	7.5



Fig. 1 Devices for the acceleration measurement

50 samples/s (0.02 s/samples) taking into account expected values, during 10 s.

The *Logger Pro* software provides a graphical and tabulated record of accelerations based on time, obtained during the duration of the study. The software allows to know the resonance frequencies of the system from a acceleration record by applying FFT to those data. Through this tool, the time domain signal is transformed to the frequency domain and it is possible to evaluate the frequency content of the analyzed signal.

2.3 Load-displacement test

After physical measurements were taken and recorded, cantilever bending tests were carried out according to the procedures of the American standard ASTM-D1036 [3] which were also adopted by the Argentinian standard IRAM 9529 [13]. The goal of this experiment was to determine the values of modulus of elasticity to be used in the numerical calculation as reference (see, Sect. 3.4). Each pole was placed in the testing setup so that its ground line coincided with the front face of the crib. The ground line distance from base was at least 15% of the length of the shortest pole and at 5 m from the tip and the loading point at 0.6 m from the tip in all cases. Load was applied by means of a winch capable of pulling at a constant rate of speed. The winch was set far enough from the pole so that the small angle between the initial and the final position of the pulling line may be disregarded, at distances N and M indicated in the standard [3], being, in this case, 4.7 m and 33.5 m, respectively. A schematic diagram of test setup may be appreciated in Fig. 2, and a image of the test setup can be observed in Fig. 3.

The load was measured by means of a dynamometer of suitable capacity (5 kN) placed in the pulling line and

graduated in 0.04 kN. Deflections at the loading point in the direction perpendicular to the initial pole axis t were measured by means of a tape capable of registering 1 mm and a datum board was also utilized for facilitating the measurements. The displacements s in the direction of the axis of the pole were registered to perform the correction of the applied load and take only the perpendicular to the original axis of the pole component. A minimum of 15 simultaneous readings of deflection and load were taken at intervals of the load equal to 0.1 kN. The pole to be tested was fixed from the bottom end to ground line in a crib. The crib was built in such a manner that the movement of the lower end of pole during the test was minimized. The displacements at g_1 and g_2 points on the crib were recorded to make the correction of t by vertical and rotational motion in the ground line.

A first type of modulus of elasticity (MOE_S) was determined with the equation adopted by the American standard mentioned before [3], as follows:

$$MOE_S = \frac{4L^3P}{3\pi\Delta A^3B} [\text{MPa}], \quad (1)$$

where L is the length from the ground line to the loading point (mm), P is the increment of load on the straight line portion of the load-displacement curve (N), Δ is the increment of displacement corresponding to P and corrected for displacement at the support point (mm), A is the radius of the pole at the ground line (mm), and B is the radius of the pole at the loading point (mm).

Also, the maximum fiber stress at the ground line (F) for each pole was calculated as follows:

$$F = \frac{32\pi^2P(L - \Delta L)}{C^3} [\text{MPa}], \quad (2)$$

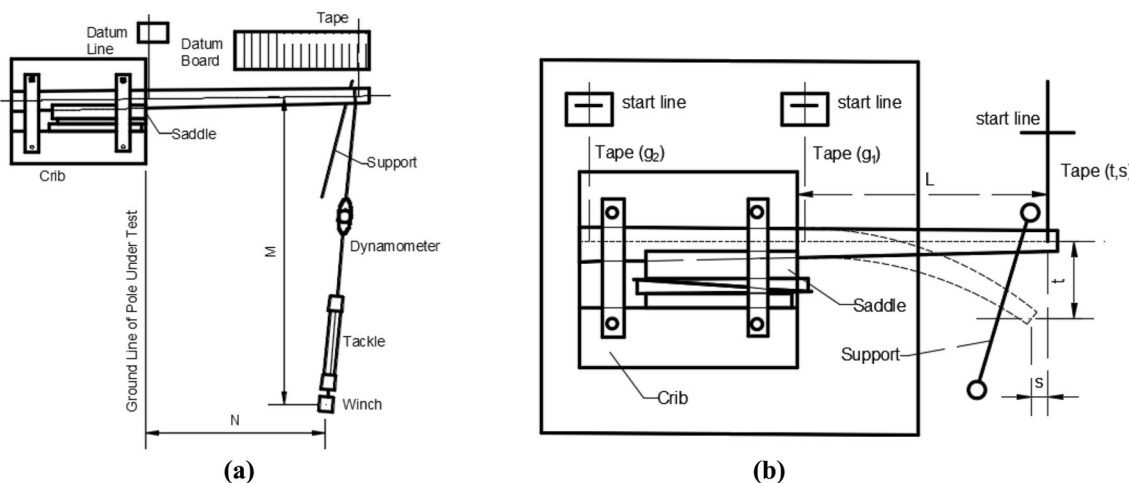


Fig. 2 Schematic layout of field mechanical test of wooden poles: **a** general scheme [3], **b** detail of record for correction of translation and rotation at the clamping system [13]



Fig. 3 Load-displacement test setup

where ΔL is the longitudinal deflection of the load point at the maximum load (mm), and C is the circumference at ground line (mm).

2.4 Density and moisture tests

The moisture content and density were determined according to the procedures established in ISO 3130 [14] and ISO 3131 [15], respectively, using a knot-free disk taken from the proximity of the fixing point after the static test. The specimens were obtained by sawing pole slices in the area to the ground line, cutting cubes of approximately 50 mm of edge. The dimensions of each test piece were taken with an accuracy of 0.05 mm in wet and anhydrous state after oven drying. The weight was recorded with a digital scale at 0.1 gr of accuracy.

The moisture content was determined according to ISO 3130 [14]. By weight difference, the mass loss of the test pieces in the initial state to their anhydrous state was calculated. To achieve this last condition, the test pieces were placed in an oven at $103^{\circ}\text{C} \pm 2^{\circ}\text{C}$ for at least 24 hours until constant weight (Fig. 4). In this state, both the weight and volume were determined, then the moisture content and the dry density were calculated.

2.5 Numerical models

The numerical model consisted of a Euler beam clamped at the ground line (cantilever beam) and subjected to a load at 0.6 m from the free tip, with the geometry according to the recorded data (main measures depicted in Table 1) and taking into account the knots and cracks (more details will be included below in Sect. 3.1), and properties of the material previously determined by the corresponding standards ([3, 14, 15]). The load at the tip was taken equal to that registered at each point of displacement in the experimental test, to emulate the displacements at the point of application of the load and compare with the measured results.

A numerical modal analysis was carried out to obtain the natural frequencies, which were then compared with the outcomes of the corresponding test. The software used was the FlexPDE7 [16] based on a finite elements discretization, with 50 quadratic type elements, and the results were processed with the Matlab software [17].



Fig. 4 Drying of the wood samples **a** oven and **b** samples with their position in the trunk of pole

3 Results

Results of the visual survey, density determination, calculation of MOE and natural frequencies are reported herein. On the other hand, some of these results are compared with values from these and other authors.

In Table 2, the results of the load-displacement test, density, moisture and knots and cracks rate for each pole are summarized. The value of MOE_S is the proposed by the standard [3], according to the Eq. 1, and it is based on the load-displacement records. $SuKR_{max}$ and $SuCR_{max}$ are the maximum rates of knots and cracks for each 0.45 m length section of each pole.

3.1 Records of knots and cracks

In Fig. 5, the recorded knots and cracks are shown graphically. On the X axis, the measurements on the circumference with respect to a proposed longitudinal axis of reference are indicated. The Y axis goes from the ground line to the applied load point. It should be noted that the two axes scales are different. The blue lines indicate the circumference values along each pole. The knots are represented by the red and black points where their size indicate the observed dimensions. The red points represent knots that reach the surface, and the black points, knots that do not reach the surface, but are visible as protuberances. The magenta lines indicate the position of the cracks and their thickness is representative of the registered width.

In Fig. 6, it is shown how the visible knots (A), the knots that do not reach surface or hidden knots (B), and the cracks (C) were registered. The reference axis adopted along the pole (D) is also indicated.

Regarding the values $SuKR$ (Table 2), the size of the sample is not sufficient to establish a relationship between

Table 2 Summary of the results of the tests carried out on the poles

Pole	MOE_S (MPa)	ρ (kg/m ³)	$\rho_{12\%}$ (kg/m ³)	W (%)	$SuKR_{max}$	$SuCR_{max}$
1	10004	580	535	29	0.41	0.00
2	11902	653	608	27	0.31	0.04
3	11907	580	543	26	0.32	0.02
4	10315	550	511	28	0.21	0.03
5	9314	578	531	30	0.25	0.05
6	14597	750	714	22	0.28	0.03

ρ basic density at W% of moisture content

$\rho_{12\%}$ reference density at 12% of moisture content

W moisture content

the knots rate and the value of MOE, however, with the values representing the proportion of cracks $SuCR$, it is observed that the pole with the lowest MOE is the one with a higher ratio of $SuCR$.

3.2 Experimental determination of the modulus of elasticity (MOE)

Fig. 7 shows the results of the load-displacement test for all the poles. Based on these values and in accordance with the ASTM standard [3], the MOE values for each one were calculated. These values are shown in the first column of the Table 2.

In Fig. 8, the stress-strain values are shown, calculated according to Eq. 2.

The found values were then compared with those obtained by Torran [7], who carried out experiments on new, green and untreated poles of the same species, and obtained an average value of 10935 MPa with a coefficient of variation (COV) equal to 14%. The values in the Table 2 are practically within the 60% of probability of a normal distribution, except for the MOE of the healthy pole (Pole 6).

3.3 Density and moisture

After carrying out the tests described in Sect. 2.4, density and moisture values at the moment of each test were obtained. They are shown in column 3 and 5 of Table 2.

These density values were corrected for the 12% of moisture (column 4 of Table 2). When compared to a characteristic value $\rho_{0.05} = 430 \text{ kg/m}^3$, it is seen that the corrected density values are higher even when the pole is deteriorated. $\rho_{0.05}$ is the wood density with 12% of moisture, corresponding to the 5th percentile suggested by the standard [18].

With respect to the MOE values in relation to moisture, it should be noted that the test pieces with higher moisture value correspond to the poles with greater deterioration. The highest moisture value corresponded to the pole with the lowest MOE value, and the minimum moisture corresponded to the new pole that had the highest MOE value. The poles with deterioration were those with the lower density value, which would indicate that the deterioration over the material properties is more severe than mechanical defects' incidence (cracks).

3.4 Numerical determination of MOE and comparison with MOE from standard

The cross-section of the poles did not have uniform variation along the length, so it was assumed that there

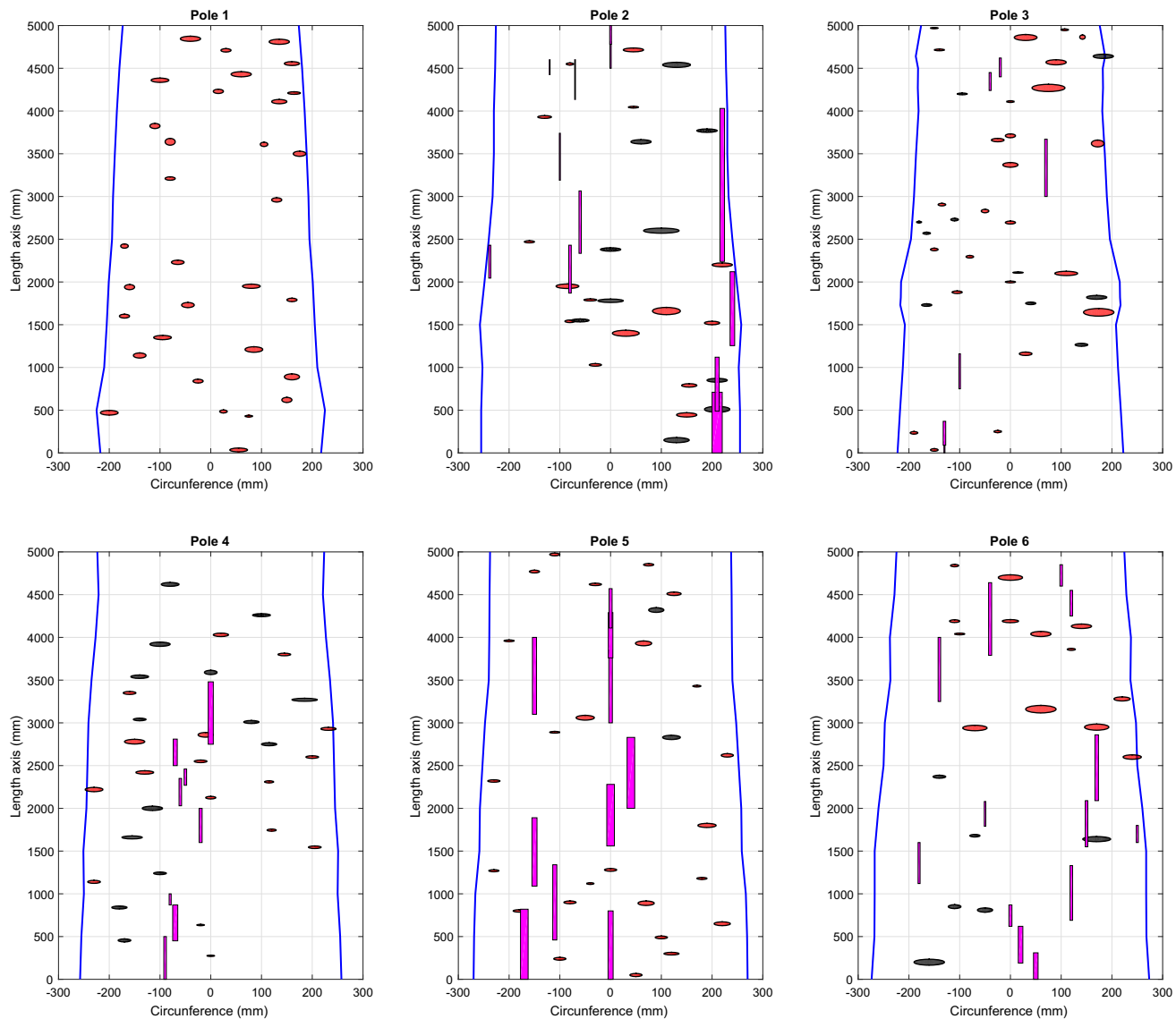


Fig. 5 Record of knots and cracks from visual survey: visible knots (red points), hidden knots (black points), cracks (magenta lines) and circumference limits (blue lines) (colour figure online)



Fig. 6 Record of visible knots (a), hidden knots (b), cracks (c) and the reference line (d)

was a difference between the MOE proposed by the standard [3] and that which the material would have. For this reason, in addition to the value proposed by the

standard MOE_S , other MOE values were determined. These are detailed below:

- MOE_S : according to the expression of the ASTM Standard [3];
- MOE_R : by numerical approximation taking into account the real measured geometry;
- MOE_K : by numerical approximation taking into account the presence of knots;
- MOE_C : by numerical approximation taking into account visible cracks;
- MOE_D : by numerical approximation taking into account all defects registered.

Since MOE_S is a general value that does not take into account geometries different from a truncated cone, as well

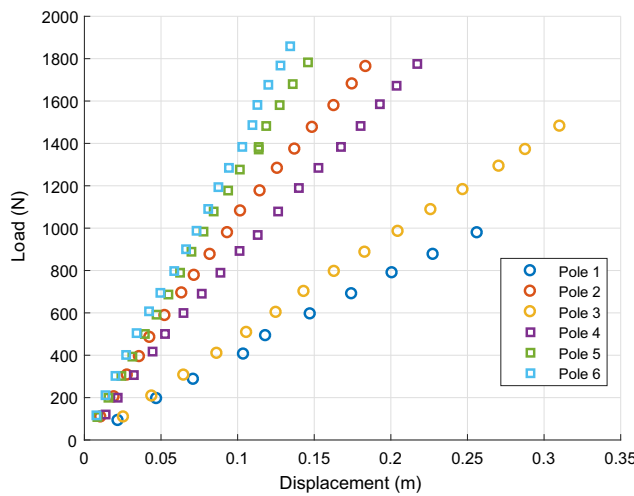


Fig. 7 Results of the load-displacement test

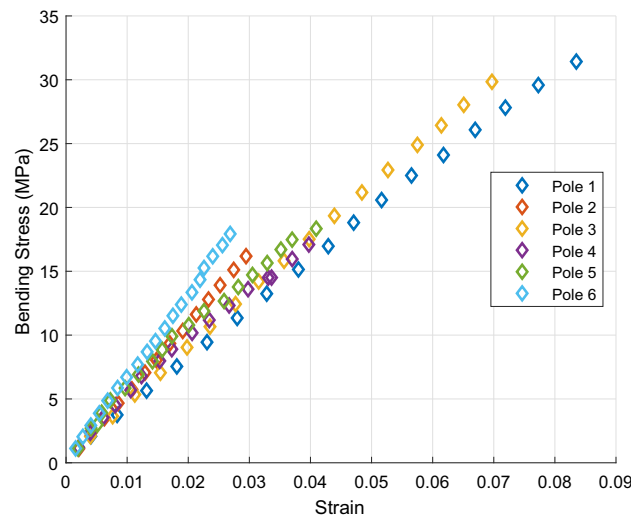


Fig. 8 Stress–strain curves obtained from the experiments

as cracks, knots, etc., it is necessary to determine an adjusted MOE for each different case. Here, each numerical model was run until a target displacement was obtained. The resulting values of MOE are reported in Table 3. As a result, the found MOE of a pole with deterioration is greater than the same pole free of defects. For instance, the values corresponding to MOE_D for all the

poles are greater than the MOE_R since the pole with all the defects needs a larger MOE (adjusted value) to achieve the same displacement.

There is a difference between the MOE values with respect to the value suggested by the standard [3] in the order of 6% with respect to the healthy poles. The difference is larger for specimens with more irregular geometry. Since MOE_S is lower, its use in the numerical calculations would lead to conservative results.

The presence of cracks in the poles does not indicate significant differences when the second moment of area is corrected. It is found that the crack influence in the results is minimum.

3.5 Experimental and numerical natural frequencies comparison

The values of natural frequencies were determined with an impact test on each pole prior to the corresponding load-displacement test. On the other hand, the density values of each pole obtained and described in Sect. 3.3, and the MOE values calculated in the Sect. 3.4 were introduced in the numerical models of the cantilever beam to determine the values of the first three vibration frequencies and compare them with the experimental measurements. As a verification, the theoretical frequencies of truncated cone elements were calculated according to [19] with the values of geometry and material properties measured in the experimental stage. The truncated cone geometry was derived from the measures of Table 1, using the MOE_S and the mean density from Table 2, columns 2 and 3, respectively.

In Fig. 9, as an example, the results of a deteriorated and a new pole are shown. In both cases (Fig. 9a, b), the first frequency of vibration calculated with all proposed numerical models (vertical lines) matches very closely with the value measured experimentally. Higher frequencies exhibit more discrepancy among the numerical and experimental results, being different more pronounced for the third one. The higher is the frequency, the more sensitive it is to parameters such as the density and MOE.

The materialization of a perfect embedment is practically unattainable in both the laboratory setup as well as in real utility poles. It is apparent that this issue deserves a further study such as the consideration of the elasticity of the clamped end as a uncertain variable.

The percentage differences between the results found with MOE_S and MOE_C (see Fig. 9, \times and $+$ symbols, respectively) in the case of the pole 5 are: -7% , -6% and -6% , from the first, second and third frequency, respectively. In general, the differences are small for all cases.

Table 3 Adjusted MOE values for each pole (MPa)

Pole	MOE_S	MOE_R	MOE_K	MOE_C	MOE_D
1	10004	10664	11549	10664	11549
2	11902	12106	12476	12291	12369
3	11907	12835	13946	12862	13974
4	10315	10603	10751	11175	12415
5	9314	10695	11108	11270	11271
6	14597	15263	15793	15115	15891

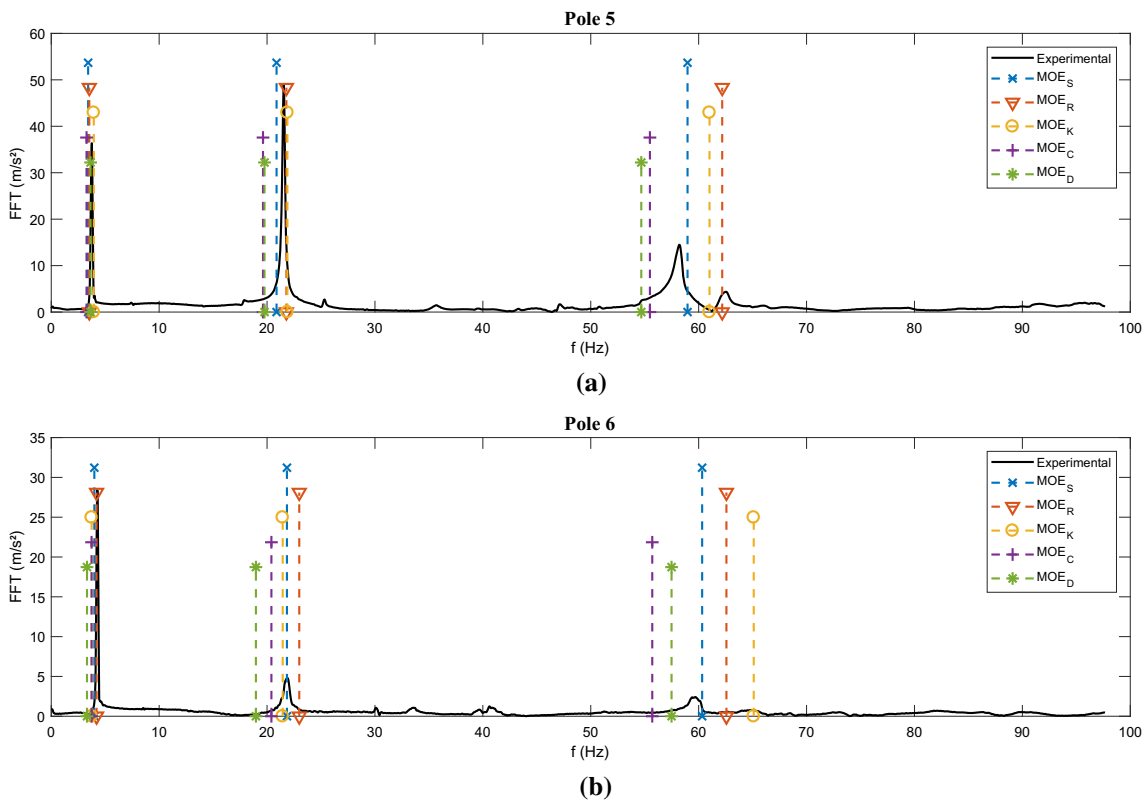


Fig. 9 Frequencies spectrum. **a** deteriorated pole 5; **b** healthy pole 6

As mentioned in Sect. 3.3, the deterioration of the material causes an appreciable variation of the density, with respect to the healthy wood. According to the standards recommendations [14, 15], the wood mass density determination implies a destructive test. That is, this data is not usually available for poles in service. To assess the influence of mass density on the frequency values, numerical results were found for all the MOE alternatives in the case of pole 5 but setting the mass density of the healthy pole 6 (all others parameters are kept fixed). These results are shown in Fig. 10. By comparing the plots of Figs. 9a and 10, the effect of mass density on the frequencies values with and without deterioration is apparent.

To make this issue clearer, Table 4 depicts the corresponding numerical values of the frequencies. It was clear that the use of the healthy pole mass density leads to lower values of frequencies.

4 Conclusions

A study to evaluate the deterioration of wood utility poles was presented. The objective was to find a correspondence between the degree of deterioration of the wood and the recorded frequencies. Both experimental tests and numerical simulations were carried out. A sample of six

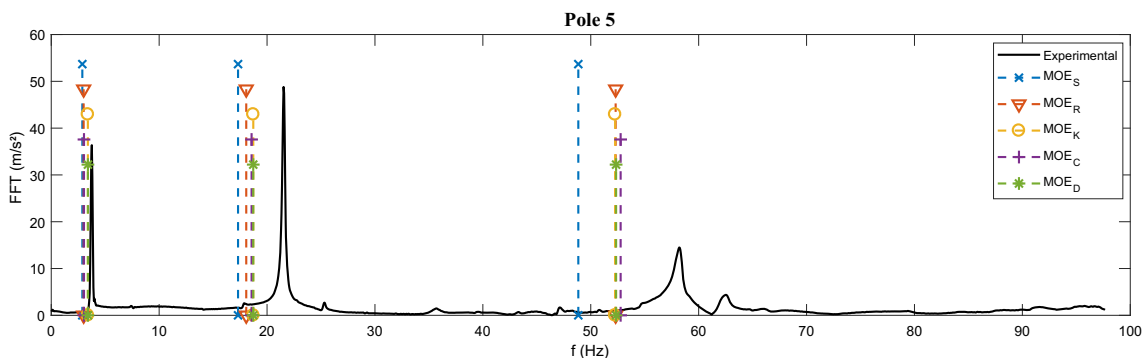


Fig. 10 Frequency spectrum. Pole 5. Numerical natural frequencies found with healthy pole mass density

Table 4 Numerical natural frequencies of the pole 5 using the deteriorated (ρ_D) and the healthy pole mass density (ρ_H)

	1 st freq (Hz)		2 nd freq (Hz)		3 rd freq (Hz)	
	w/ ρ_D	w/ ρ_H	w/ ρ_D	w/ ρ_H	w/ ρ_D	w/ ρ_H
MOE _S	3.41	2.88	20.88	17.31	58.97	48.85
MOE _R	3.53	3.00	21.79	18.07	62.18	52.31
MOE _K	3.94	3.39	21.89	18.72	61.00	52.26
MOE _C	3.27	3.03	19.63	18.57	55.48	52.77
MOE _D	3.64	3.40	19.76	18.72	54.68	52.35
Exper.	3.76		21.53		58.20	
Theoret.	4.07		23.52		64.32	

Comparison with experimental [3] and theoretical [19] values

ρ_D and ρ_H values are detailed in Table 2

Eucalyptus grandis poles was employed, five of them with different degrees of deterioration after a period of service and a new one, without use.

First, a visual survey was performed to obtain information about the knots, cracks and external geometry. Also, the density was determined after the drying of samples from each pole. Load-displacement tests were carried out and the values of MOE were determined using the standard rules. Dynamic experiments allowed to find the natural frequencies.

On the other hand, numerical models were employed with different variants, taking into account the real geometry, presence of knots, visible cracks, and the defects, which were used to determine MOE values (Table 3). It was found that the wood of the deteriorated poles has lower density, higher moisture and lower MOE values than the wood of the new pole. This properties variation influences the vibration frequencies. A comparison between the frequency spectrum found from the experiments with the values of frequencies obtained with five numerical model with different MOE values, was reported. A very close agreement was found for the fundamental frequency. Some discrepancies were observed as the frequency index increases.

Another comparison was made to determine the importance of considering deteriorated versus healthy wood density values in the frequency estimation. As an illustration, two models of a deteriorated pole with its geometry characteristics and MOE value, one with deteriorated wood density value and another, with healthy one were performed. It was concluded that significant errors would be included if the healthy wood density were employed to estimate the frequency values. These errors get larger as the index increases.

A perfect clamped end is not feasible neither in the laboratory nor in the real pole site. A further study considering the boundary elasticity as a random variable would be useful.

It is possible to make a qualitative estimate of the state of the deterioration and make decisions about the permanence or replacement necessity from the geometry data, MOE and healthy wood density and from the first two frequencies record. The availability of statistics of the new wood density would serve for this purpose. Publications such as the Argentinian standard CIRSOC 601 [18] contain information on this regard. However, in the authors' opinion, the best alternative would be to have the properties records of the poles' lot purchased by the company responsible for the poles' placement.

Acknowledgements The authors acknowledge the financial support of the Department of Engineering, the SGCyT-Universidad Nacional del Sur, CIC-Bs.As., ANPCyT and CONICET, all Argentinian agencies.

References

- ASTM D 143-94 (2007) Standard test methods for small clear specimens of timber. West Conshohoken.
- ASTM D 198 (2002) Standard test methods of static test of lumber in structural sizes. West Conshohoken.
- ASTM D 1036 (2005) Standard test methods of static test of wood poles. West Conshohoken.
- Piter J, Zerbino R, Blaß H (2004) Visual strength grading of Argentinean eucalyptus grandis. Holz als Roh-und Werkst 62(1):1–8
- García DA, Rosales MB (2017) Deflections in sawn timber beams with stochastic properties. Eur J Wood and Wood Prod 75(5):683–699
- García DA, Sampaio R, Rosales MB (2015) Vibrational problems of timber beams with knots considering uncertainties. J Braz Soc Mech Sci Eng 38:1–13
- Torrán E, Zitto S, Cotrina A, Piter JC (2009) Bending strength and stiffness of poles of Argentinean eucalyptus grandis. Maderas. Ciencia y Tecnología 11(1):71–84
- Kurz JH (2015) Monitoring of timber structures.
- Yu Y, Li J, Yan N, Dackermann U, Samali B (2016) Load capacity prediction of in-service timber utility poles considering wind load. J Civil Struct Health Monit 6(3):385–394
- Shafieezadeh A, Onyewuchi UP, Begovic MM, DesRoches R (2014) Age-dependent fragility models of utility wood poles in power distribution networks against extreme wind hazards. IEEE Trans Power Deliv 29(1):131–139
- ANSI-05.1 (2002) American national Standard for wood poles—Specifications and dimensions. Washintong.
- Vernier Software and Technology (2010) “LabQuest TM.” <https://www.vernier.com/products/interfaces/>.
- IRAM 9529 (2005) Wood poles static flexion test methods (Spanish). Buenos Aires.
- ISO 3130:1975 (1975) Wood—determination of moisture content for physical and mechanical test. Geneva.
- ISO 3131:1975 (1975) Wood—Determination of density for physical and mechanical tests.
- FlexPDE, PDE (2017) Solutions inc.. <http://www.pdesolutions.com>.
- MathWorks, Inc. MATLAB (2011) Matlab 2011a.
- CIRSOC 601 (2011) Proyecto de Reglamento Argentino de Estructuras de Madera (Spanish).
- Conway H, Becker E, Dubil J (1964) Vibration frequencies of tapered bars and circular plates. J Appl Mech 31(2):329–331

Terms and Conditions

Springer Nature journal content, brought to you courtesy of Springer Nature Customer Service Center GmbH (“Springer Nature”). Springer Nature supports a reasonable amount of sharing of research papers by authors, subscribers and authorised users (“Users”), for small-scale personal, non-commercial use provided that all copyright, trade and service marks and other proprietary notices are maintained. By accessing, sharing, receiving or otherwise using the Springer Nature journal content you agree to these terms of use (“Terms”). For these purposes, Springer Nature considers academic use (by researchers and students) to be non-commercial.

These Terms are supplementary and will apply in addition to any applicable website terms and conditions, a relevant site licence or a personal subscription. These Terms will prevail over any conflict or ambiguity with regards to the relevant terms, a site licence or a personal subscription (to the extent of the conflict or ambiguity only). For Creative Commons-licensed articles, the terms of the Creative Commons license used will apply.

We collect and use personal data to provide access to the Springer Nature journal content. We may also use these personal data internally within ResearchGate and Springer Nature and as agreed share it, in an anonymised way, for purposes of tracking, analysis and reporting. We will not otherwise disclose your personal data outside the ResearchGate or the Springer Nature group of companies unless we have your permission as detailed in the Privacy Policy.

While Users may use the Springer Nature journal content for small scale, personal non-commercial use, it is important to note that Users may not:

1. use such content for the purpose of providing other users with access on a regular or large scale basis or as a means to circumvent access control;
2. use such content where to do so would be considered a criminal or statutory offence in any jurisdiction, or gives rise to civil liability, or is otherwise unlawful;
3. falsely or misleadingly imply or suggest endorsement, approval , sponsorship, or association unless explicitly agreed to by Springer Nature in writing;
4. use bots or other automated methods to access the content or redirect messages
5. override any security feature or exclusionary protocol; or
6. share the content in order to create substitute for Springer Nature products or services or a systematic database of Springer Nature journal content.

In line with the restriction against commercial use, Springer Nature does not permit the creation of a product or service that creates revenue, royalties, rent or income from our content or its inclusion as part of a paid for service or for other commercial gain. Springer Nature journal content cannot be used for inter-library loans and librarians may not upload Springer Nature journal content on a large scale into their, or any other, institutional repository.

These terms of use are reviewed regularly and may be amended at any time. Springer Nature is not obligated to publish any information or content on this website and may remove it or features or functionality at our sole discretion, at any time with or without notice. Springer Nature may revoke this licence to you at any time and remove access to any copies of the Springer Nature journal content which have been saved.

To the fullest extent permitted by law, Springer Nature makes no warranties, representations or guarantees to Users, either express or implied with respect to the Springer nature journal content and all parties disclaim and waive any implied warranties or warranties imposed by law, including merchantability or fitness for any particular purpose.

Please note that these rights do not automatically extend to content, data or other material published by Springer Nature that may be licensed from third parties.

If you would like to use or distribute our Springer Nature journal content to a wider audience or on a regular basis or in any other manner not expressly permitted by these Terms, please contact Springer Nature at

onlineservice@springernature.com